

# Combined Analysis of C-18 Unsaturated Fatty Acids Using Natural Abundance Deuterium 2D NMR Spectroscopy in Chiral Oriented Solvents

Philippe Lesot,<sup>\*,†</sup> Vincent Baillif,<sup>‡</sup> and Isabelle Billault<sup>‡</sup>

Université de Paris-Sud (XI), ICMO, UMR CNRS 8182, Laboratoire de Chimie Structurale Organique, Equipe de RMN en Milieu Orienté, UFR des sciences d'Orsay, Bât. 410, 91405 Orsay Cedex, France, and Université de Nantes, CEISAM, Chimie Et Interdisciplinarité, Synthèse, Analyse, Modélisation, UMR CNRS 6230, UFR des Sciences et des Techniques, 2, rue de la Houssinière, BP 92208, 44322 Nantes Cedex 3, France

The quantitative determination of isotopic ( $^2\text{H}/^1\text{H}$ )<sub>i</sub> ratios at natural abundance using the SNIF-NMR protocol is a well-known method for understanding the enzymatic biosynthesis of metabolites. However, this approach is not always successful for analyzing large solutes and, specifically, is inadequate for prochiral molecules such as complete essential unsaturated fatty acids. To overcome these analytical limitations, we use the natural abundance deuterium 2D NMR (NAD 2D NMR) spectroscopy on solutes embedded in polypeptide chiral liquid crystals. This approach, recently explored for measuring ( $^2\text{H}/^1\text{H}$ )<sub>i</sub> ratios of small analytes (Lesot, P.; Aroulanda, C.; Billault, I. *Anal. Chem.* 2004, 76, 2827–2835), is a powerful way to separate the  $^2\text{H}$  signals of all nonequivalent enantioisotopomers on the basis both of the  $^2\text{H}$  quadrupolar interactions and of the  $^2\text{H}$  chemical shift. Two significant advances over our previous work are presented here and allow the complete isotopic analysis of four mono- and polyunsaturated fatty acid methyl esters: methyl oleate (1), methyl linoleate (2), methyl linolenate (3), and methyl vernoleate (4). The first consists of using NMR spectrometers operating at higher magnetic field strength (14.1 T) and equipped with a selective cryoprobe optimized for deuterium nuclei. The second is the development of *Q*-COSY Fz 2D NMR experiments able to produce phased  $^2\text{H}$  2D maps after a double Fourier transformation. This combination of modern hardware and efficient NMR sequences provides a unique tool to analyze the ( $^2\text{H}/^1\text{H}$ )<sub>i</sub> ratios of large prochiral molecules (C-18) dissolved in organic solutions of poly( $\gamma$ -benzyl-L-glutamate) and requires smaller amounts of solute than previous study on fatty acids. For each compound (1–4), all  $^2\text{H}$  quadrupolar doublets visible in the 2D spectra have been assigned on the basis of  $^2\text{H}$  chemical shifts, isotopic data obtained from isotropic quantitative NAD NMR, and by an interspectral comparison of the anisotropic NAD spectra of four fatty acids. The NMR results are discussed in terms of ( $^2\text{H}/^1\text{H}$ )<sub>i</sub> isotopic distribution and molecular orientation in the mesophase. For the first time, we show that the investigation of natural isotopic

fractionation of complete fatty acids is possible without the need of chemical modifications, hence providing an alternative method to probe the mechanisms of enzymes implied in the biosynthetic pathway of unsaturated fatty acids.

Unsaturated fatty acids are essential metabolites involved both as structural components of cell membranes and as active molecules in a number of biological processes.<sup>1</sup> The diversity in the classes of fatty acids is due to the large number of enzymatic modifications of their chain (introduction of double bond or triple bond, conjugated double bond, hydroxylation, epoxidation, etc.). Such reactions are known to involve small changes in the activity of enzymes of the same family (the fatty acid desaturase (FAD) superfamily) for which the mechanisms are not completely elucidated or are still unknown.<sup>2–4</sup> Quantitative  $^2\text{H}$  NMR spectroscopy in isotropic solvent is a well-known method for analyzing the natural fractionation of bioproducts<sup>5–7</sup> and kinetic or physical isotope effects.<sup>8,9</sup> Applied to fatty acid analysis, the method has provided considerable information about the mechanism of these enzymes, which are membrane-bound and difficult to isolate and study by classical approaches.<sup>10–14</sup> However, the measurement of

\* To whom correspondence should be addressed. Tel.: +33 (0)1 69 47 59. Fax: +33 (0)1 69 15 81 05. E-mail: philesot@icmo.u-psud.fr.

<sup>†</sup> Université de Paris-Sud (XI).

<sup>‡</sup> Université de Nantes.

- (1) Behrouzian, B.; Buist, P. H. *Curr. Opin. Chem. Biol.* 2002, 6, 577–582.
- (2) Behrouzian, B.; Buist, P. H. *Phytochem. Rev.* 2003, 2, 103–111.
- (3) Buist, P. H. *Tetrahedron: Asymmetry* 2004, 15, 2779–2785.
- (4) Reed, D. W.; Savile, C. K.; Qiu, X.; Buist, P. H.; Covello, P. S. *Eur. J. Biochem.* 2002, 269, 5024–5023.
- (5) (a) Martin, G.; Martin, M. *Tetrahedron Lett.* 1981, 22, 3525–3528. (b) Martin, G.; Zhang, B. L.; Naulet, N.; Martin, M. *J. Am. Chem. Soc.* 1986, 108, 5116–5122.
- (6) Schmidt, H.-L.; Werner, R.; Eisenreich, W. *Phytochem. Rev.* 2003, 2, 61–85.
- (7) Robins, R.; Billault, I.; Duan, J. R.; Guiet, S.; Pionnier, S.; Zhang, B.-L. *Phytochem. Rev.* 2003, 2, 87–102.
- (8) Singleton, D. A.; Thomas, A. A. *J. Am. Chem. Soc.* 1995, 117, 9357–9358.
- (9) Zhang, B.-L.; Jouitteau, C.; Pionnier, S.; Gentil, E. *J. Phys. Org. Chem.* 2002, 106, 2983–2988.
- (10) Billault, I.; Guiet, S.; Mabon, F.; Robins, R. *ChemBioChem* 2001, 2, 425–431.
- (11) Duan, J. R.; Billault, I.; Mabon, F.; Robins, R. *ChemBioChem* 2002, 3, 752–759.

the deuterium/hydrogen ( $^2\text{H}/^1\text{H}$ )<sub>*i*</sub> ratio by quantitative  $^2\text{H}$  NMR spectroscopy in liquids possesses two analytical limitations: (i) the rather small chemical shift dispersion of deuterium nuclei in isotropic NMR; (ii) no spectral discrimination between the enantiotopic deuterons.<sup>15</sup> These two restrictions preclude the quantification of isotopic fractionation on methylene prostereogenic sites of prochiral molecules such as C-18 saturated or unsaturated fatty acids.

To overcome these difficulties, we have recently proposed the use of natural abundance deuterium 2D NMR (NAD 2D NMR) applied to solutes dissolved in weakly orienting, chiral liquid crystals (CLCs).<sup>15–19</sup> By analyzing the case of 1,1'-bis(phenylthio)-hexane (BPTH), a fragment of methyl linoleate **2** (structures shown in Figures 1 and 7a), we demonstrated that the ( $^2\text{H}/^1\text{H}$ )<sub>*pro-R*</sub> and ( $^2\text{H}/^1\text{H}$ )<sub>*pro-S*</sub> ratios at site *i* along the chain could be measured at the same prostereogenic methylene position.<sup>15,16</sup>

To further demonstrate the potency of this method, we have investigated several complete fatty acids for two reasons: (i) to test efficiency of the method when applied to long flexible molecules;<sup>20</sup> (ii) to avoid the risk of introducing a non-natural fractionation in the chain during chemical modification of the fatty acids.<sup>10,11</sup>

To date, the  $^2\text{H}$  NMR analysis of complete fatty acids has not been performed in anisotropic solvents. To succeed in this objective, two advances in experimental conditions were required: (i) the improvement of the sensitivity of NAD experiments by increasing the signal-to-noise (S/N) ratio; (ii) the development of autocorrelation deuterium 2D experiments able to produce phased 2D spectra after the double Fourier transformation. The first condition can be addressed by using modern NMR spectrometers either operating at very high magnetic field strength or equipped with cryogenic NMR probes. A cryogenically cooled probe (cryoprobe) is a recent technology allowing a considerable reduction of electronic noise, thus providing a significant gain of sensitivity (factors 4–6) compared with classical NMR probes.<sup>21,22</sup> Obviously, the combination of both technologies offers major progress in terms of efficacy of the method. In this study, we have used a 14.1-T NMR spectrometer (92.1 MHz for  $^2\text{H}$ ) equipped with a 5-mm cryoprobe optimized for  $^2\text{H}$  nuclei. With this tool, it is possible to record anisotropic NAD NMR spectra of compounds of molecular mass over 300 g/mol, with very good S/N ratio or reasonable experimental time (overnight or less). The second

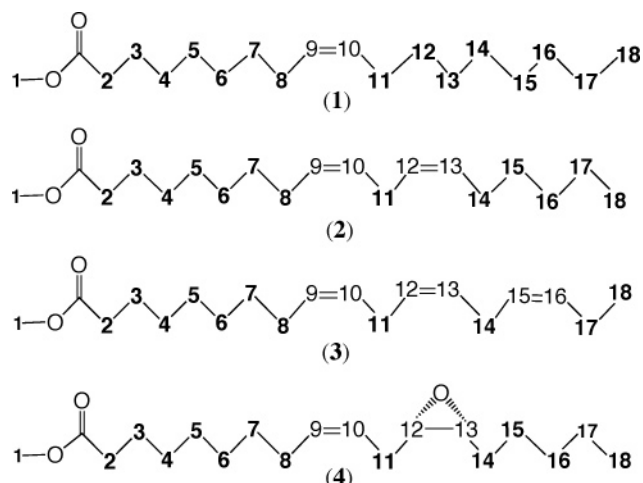


**Figure 1.** Chemical structures of FAMES 1–4 showing the atom numbering system.

condition was the development of *Q*-COSY NMR Fz and *Q*-resolved Fz experiments able to provide phased NAD maps in both dimensions with a considerable noticeable reduction of peak line widths, thus allowing the analysis of very congested NAD spectra.<sup>23</sup> (pulse sequences shown in Figure SI-1 in Supporting Information, SI).

In the current work, we have studied four C-18 unsaturated fatty acid methyl esters (FAMES) using NAD 2D NMR in chiral mesophases made of poly( $\gamma$ -benzyl-L-glutamate) (PBLG) and chloroform. The unsaturated FAMES chosen are methyl oleate (**1**), methyl linoleate (**2**), methyl linolenate (**3**), and methyl vernoleate (**4**) (Figure 1). Note that the botanical origin of **2** and the BPTH investigated previously are identical.<sup>10,15,16</sup>

First, we will focus on methyl linoleate (**2**), an essential fatty acid from which a large number of fatty acid are biosynthesized such as vernoleate, linolenate, and conjugated linolenate. The NAD NMR results obtained from **2** are discussed in terms of enantiomeric discrimination, quantitative ( $^2\text{H}/^1\text{H}$ )<sub>*i*</sub> ratios measurements, and assignment of enantiomeric isotopomers (*R* and *S*). Second, the combined analysis of NAD 2D NMR spectra recorded from **1**, **3**, and **4** in the same conditions as **2** will be discussed in terms of molecular orientational behavior.

## THEORETICAL ASPECTS

Proton decoupled deuterium NMR ( $^2\text{H}\{-^1\text{H}\}$  NMR) in CLC's is much more informative than NMR in liquid because the signals of two enantiomers or enantiotopic elements in prochiral molecules can be spectrally discriminated on the basis of  $^2\text{H}$  quadrupolar splitting differences,  $|\Delta\nu_{\text{Q}}^R - \Delta\nu_{\text{Q}}^S|$ , where:<sup>17–19</sup>

$$\Delta\nu_{\text{Q}i}^{\text{Sor}R} = \frac{3}{2}K_{\text{C-D}i} S_{\text{C-D}i}^{\text{Sor}R} \quad \text{with} \quad K_{\text{C-D}i} = \frac{e^2 Q_{\text{D}i} q_{\text{C-D}i}}{h} \quad (1)$$

$S_{\text{C-D}i}^{\text{Sor}R} = \langle 3 \cos^2(\theta_{\text{C-D}i}^{\text{Sor}R}) - 1 \rangle / 2$  defines the local order parameter and  $\theta_{\text{C-D}i}^{\text{Sor}R}$  is the angle between the C–D<sub>*i*</sub> axis for the *R* or *S* isomers relative to the magnetic field axis.  $K_{\text{C-D}i}$  is the quadrupolar coupling constant of the *i*th deuteron.

- (12) Guet, S.; Robins, R. J.; Lees, M.; Billault, I. *Phytochemistry* **2003**, *64*, 227–233.  
 (13) Billault, I.; Mantle, P. G.; Robins, R. J. *J. Am. Chem. Soc.* **2004**, *126*, 3250–3256.  
 (14) Billault, I.; Duan, J.-R.; Guet, S.; Robins, R. J. *J. Biol. Chem.* **2005**, *280*, 17645–17651.  
 (15) Lesot, P.; Aroulanda, C.; Billault, I. *Anal. Chem.* **2004**, *76*, 2827–2835.  
 (16) Baillif, V.; Robins, R. R.; Billault, I.; Lesot, P. *J. Am. Chem. Soc.* **2006**, *128*, 11180–11187.  
 (17) Lesot, P.; Merlet, D.; Loewenstein, A. J.; Courtieu, J. *Tetrahedron: Asymmetry* **1998**, *9*, 1871–1881.  
 (18) Sarfati, M.; Lesot, P.; Merlet, D.; Courtieu, J. *Chem. Commun.* **2000**, 2069–2081, and references therein.  
 (19) Lesot, P.; Sarfati, M.; Courtieu, J. *Chem. Eur. J.* **2003**, *9*, 1724–1745.  
 (20) Lesot, P.; Sarfati, M.; Merlet, D.; Ancian, B.; Emsley, J. W.; Timimi, B. A. *J. Am. Chem. Soc.* **2003**, *125*, 7689–7695.  
 (21) Kovacs, H.; Moskau, D.; Spraul, M. *Prog. NMR Spectrosc.* **2005**, *45*, 131–155.  
 (22) Lafon, O. P.; Lesot, P.; Poupko, P.; Luz, Z. *J. Chem. Phys. B* **2007**, *111*, 9453–9467.

- (23) Lafon, O.; Lesot, P.; Merlet, D.; Courtieu, J. *J. Magn. Reson.* **2004**, *171*, 135–142.

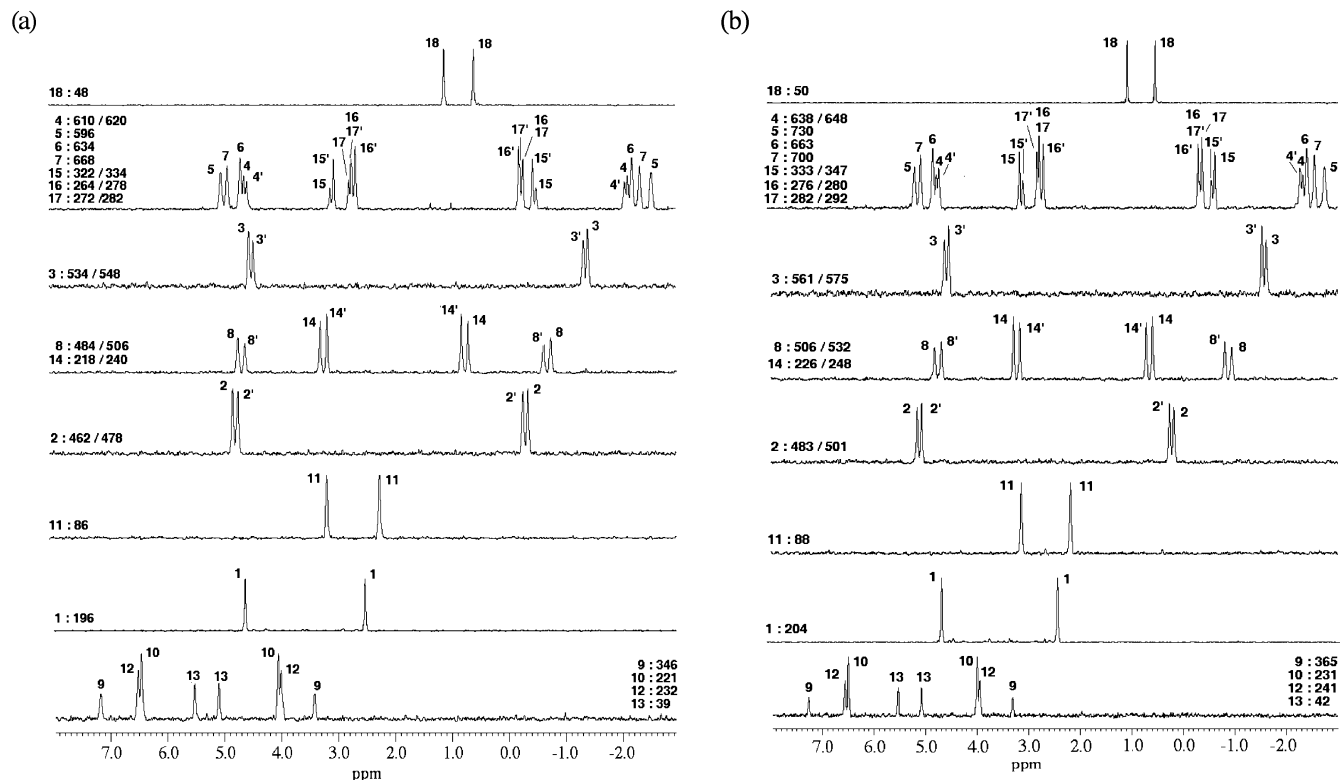


**Figure 2.**  $^2\text{H}\{-^1\text{H}\}$  1D subspectra (sum of columns) extracted from the tilted  $Q$ -COSY Fz map of **2** dissolved in (a) PBLG/ $\text{CHCl}_3$  and (b) PBDG/ $\text{CHCl}_3$ . The doublets for each nonequivalent site are noted from 1 to 18 (see Figure 1). The pair of doublet for each  $\text{CH}_2$  is noted  $x$  (outer splitting) and  $x'$  (inner splitting). The value of  $\Delta\nu_Q$ 's (reported at the side) are given in hertz. The subspectra are plotted at the same scale. Zooms of 2D maps are reported in SI. In both series, the line widths,  $\Delta\nu_{1/2}$ , vary between 2 and 5 Hz.

In the case of flexible prochiral molecules of  $C_s$  symmetry, on average on the NMR time scale enantiotopic ( $^2\text{H}$ ) nuclei in prostereogenic methylenes are also nonequivalent in CLCs because their order parameters differ ( $S_{C-Di}^{\text{pro-R}} \neq S_{C-Di}^{\text{pro-S}}$ ).<sup>24–26</sup> This occurrence makes it possible to distinguish them through their  $^2\text{H}\{-^1\text{H}\}$  NMR spectrum. Strictly defined, a  $C_s$  symmetry hydrogenated compound does not exist from the NAD NMR spectroscopy point of view because we observe a mixture of isotopomers presenting  $\text{CDH}$  groups and not  $\text{CH}_2$  ( $\text{CD}_2$ ) groups. Thus, this isotopic chirality is introduced into the molecules by virtue of the natural  $^2\text{H}/^1\text{H}$  isotopic substitution.<sup>17</sup> During the discussion, both terms “enantiotopic directions” and “enantioisotopomers” will be used without distinction.

## RESULTS AND DISCUSSION

**Study of Methyl Linoleate (2): General Approach.** The methyl ester of linoleic acid **2** possesses two double bonds located between positions 9–10 and 12–13 (Figure 2). This compound has already been extensively analyzed in isotropic NMR.<sup>10,11,14</sup> The isotropic NAD 1D spectrum of **2** recorded at 92.1 MHz is shown in Figure SI-2. As chiral mesophase, we have tested the polymer PBLG dissolved in  $\text{CHCl}_3$ . This mixture is useful for the following reasons: (i) it gives samples of low viscosity; (ii) it provides

excellent spectral discriminations; (iii) it can dissolve large amounts of solute (polar or apolar), (iv) the NAD doublet of chloroform does not interfere with the signal of **2**.

The analysis of the  $Q$ -COSY Fz 2D map after the tilt procedure (see Figure SI-3) shows that numerous  $^2\text{H}$  sites that have identical resonances in isotropic NAD NMR are now separated on the basis of their  $\Delta\nu_Q$ .<sup>19,23</sup> Notably, the ( $^2\text{H}/^1\text{H}$ ) ratios at the ethylenic sites 10 and 12 can be accessed for the first time. Previously, it was not possible to determine these ratios from isotropic NAD spectra, as they were lost during the chemical cleaving of the double bonds to produce small fragments, such as BPTH.<sup>10</sup> For a clear description of the results for **2**, Figure 2a presents all NAD 1D subspectra extracted from the tilted 2D map. The examination of the NAD data indicates that the  $\Delta\nu_Q$ 's vary between 40 and 700 Hz, but this variation is not simply related to the position of the deuterated site along the flexible chain. The largest values correspond to the deuterons in the methylene groups in positions 4–7, namely those closest to the ester function (the most polar group). As generally found independent of the class of molecules concerned, the methyl group 18 shows small quadrupolar splittings. This effect is due both to the conformational dynamics of the chain and to the averaging of  $\Delta\nu_Q$ 's of three deuterium sites resulting from free rotation of the methyl group around the  $\text{C}-\text{CH}_3$  axis.<sup>19</sup> The small magnitude of  $\Delta\nu_Q$ 's for the ethylenic deuteron 13 suggests an angle,  $\theta$ , between the  $\text{C}-\text{D}$  bond and  $\text{B}_0$  axis (see eq 1) close to the magic angle ( $\theta = \theta_m = 54.7^\circ$ ). The values of all  $\Delta\nu_Q$ 's are presented in Table SI-1.

(24) Merlet, D.; Ancian, B.; Courtieu, J.; Lesot, P. *J. Am. Chem. Soc.* **1999**, *121*, 5249–5258.

(25) Meddour, A.; Canet, I.; Loewenstein, A.; Péchiné, J. M.; Courtieu, J. *J. Am. Chem. Soc.* **1995**, *116*, 9652–9656.

(26) Merlet, D.; Emsley, J. W.; Lesot, P.; Courtieu, J. *J. Chem. Phys.* **1999**, *111*, 6890–6896.



The assignment of quadrupolar doublets has been possible by combining various sources of information: (i) the isotopic fractionations derived from previous analyses (for instance, the odd/even effect along the chain ( $^{2}\text{H}/^{1}\text{H}$ )<sub>even</sub> > ( $^{2}\text{H}/^{1}\text{H}$ )<sub>odd</sub>);<sup>10,11</sup> (ii) the kinetic isotopic effects (KIEs) already reported during the desaturation steps;<sup>27–30</sup> (iii) the  $^{2}\text{H}$  chemical shift for some prostereogenic sites determined in isotropic NAD 1D NMR spectra; (iv) the comparison of the NAD 2D NMR spectra of the other FAMES **1**, **3**, and **4** studied (see below). For example, the assignment of four doublets located at 5.3 ppm is based on the fact that  $^{2}\text{H}$  odd sites (9/13) are systematically more depleted than even sites (10/12).<sup>10,11,13,14</sup> Indeed, a normal KIE has been shown in vivo at site 12 during the action of  $\Delta^{12}$  desaturase,<sup>27,28</sup> and for some species, a KIE has also been detected at site 9 when any step other than the first CH abstraction was the kinetically limiting step.<sup>28–30</sup> Such KIEs should lead to lower ( $^{2}\text{H}/^{1}\text{H}$ )<sub>i</sub> ratios at sites 9 and 12 compared with sites 13 and 10, respectively, since the latter are not submitted to this effect. On this basis, we have assigned the quadrupolar doublets on the following basis: (i) the ( $^{2}\text{H}/^{1}\text{H}$ )<sub>9</sub> and ( $^{2}\text{H}/^{1}\text{H}$ )<sub>13</sub> ratios are lower than the ( $^{2}\text{H}/^{1}\text{H}$ )<sub>12</sub> and ( $^{2}\text{H}/^{1}\text{H}$ )<sub>10</sub> ratios (odd/even effect); (ii) the ( $^{2}\text{H}/^{1}\text{H}$ )<sub>9</sub> ratio is lower than ( $^{2}\text{H}/^{1}\text{H}$ )<sub>13</sub>; (iii) the ( $^{2}\text{H}/^{1}\text{H}$ )<sub>12</sub> ratio is lower than ( $^{2}\text{H}/^{1}\text{H}$ )<sub>10</sub> ratio (KIE). Rigorously, this attribution should be confirmed by the regioselective synthesis of **2**, isotopically enriched at positions 10 and 12. The use of the odd/even alternation has also been applied to assign quadrupolar doublets centered at ~1 ppm.

From the analysis of NAD subspectra, it appears that almost all methylene groups are spectrally enantioresolved except for sites 5, 6, 7, and 11. Additionally, for each enantioresolved site, a difference of peak intensity was noticed, either on the outer doublet, denoted  $x$  (sites 2, 3, and 8), or on the inner doublet, denoted  $x'$  (sites 14 and 15). This suggests a depletion for one of the two enantiotopic C–D directions. However, these variations could have multiple origins including the following: (i) a non-statistical isotopic distribution; (ii) different line widths for the inner and outer doublets;<sup>15</sup> (iii) conditions for a quantitative measurement of the ( $^{2}\text{H}/^{1}\text{H}$ )<sub>i</sub> ratios not fulfilled (e.g., recycling time too short).<sup>5a,31</sup>

To unambiguously assess the origin of these spectral features, two further NMR experiments were performed with the same NMR conditions as in PBLG. First, we recorded the NAD NMR 2D spectrum of **2** dissolved in an achiral oriented solvent (denoted PBG) made of an equal amount of PBLG and PBDG (enantiomer of PBLG) dissolved in  $\text{CHCl}_3$ . Second, we recorded the NAD 2D spectrum of **2** dissolved in the PBDG/ $\text{CHCl}_3$  mesophase.

In the PBG racemic mixture, no spectral enantiodiscrimination is possible, and the splitting measured for a given site is equal to the algebraic average of  $\Delta\nu_Q$ 's measured in PBLG (or PBDG).<sup>21,32</sup>

(27) Aroulanda, C.; Merlet, D.; Courtieu, J.; Lesot, P. *J. Am. Chem. Soc.* **2001**, *123*, 12059–12066.

(28) Buist, P. H.; Behrouzian, B. *J. Am. Chem. Soc.* **1998**, *120*, 871–876.

(29) Behrouzian, B.; Fauconnot, L.; Daligault, F.; Nugier-Chauvin, C.; Patin, H.; Buist, P. H. *Eur. J. Biochem.* **2001**, *268*, 3545–3549.

(30) 121) Meesapyodsuk, D.; Reed, D. W.; Cheevadhanarak, S.; Deshnum, P.; Covello, P. S. *Comp. Biochem. Physiol. Biochem. Mol. Biol.* **2001**, *129*, 831–835.

(31) Behrouzian, B.; Buist, P. H.; Shanklin, J. *Chem. Commun.* **2001**, 401–402.

(32) Martin, M. L.; Martin, G. J. In *NMR Basic Principles and Progress*; Diehl, P., Fluck, E., Günther, H., Kosfeld, R., Seeling, J., Eds.; Springer: Berlin, 1990; Vol. 23, pp 1–61.

This information is very useful to assign pairs of quadrupolar doublets associated with the same methylene group when various  $^{2}\text{H}$  signals obscure the NAD spectra. Thus, the doublet pairs from methylenes 16 and 17 could be assigned. The results obtained in PBG are shown in Figure SI-4, and the values of  $\Delta\nu_Q$  for each deuterium site are listed in Table SI-1. As no major discrepancies exist between the  $\Delta\nu_Q$ 's obtained in PBG and the average of  $\Delta\nu_Q$ 's in PBLG (or in PBDG), it appears that the signs of  $\Delta\nu_Q$ 's for *R* and *S* enantiomeric isotopomers are identical for each discriminated methylene site (positive or negative).

Using PBDG, the enantiomer of PBLG polypeptide, the chirality of the anisotropic system is inverted, and so the sense of interaction potential is opposed to that of PBLG. As a direct consequence, the various quadrupolar doublets associated with the orientation of the *S*-enantiomeric isotopomers in PBLG correspond now to the doublets of the *R*-enantiomeric isotopomers in the PBDG phase and vice versa. Experimentally, the inversion of peak intensity for enantiotopic directions discriminated in PBLG spectrum was observed on the PBDG spectrum as expected (compare Figure 2a and b). The  $\Delta\nu_Q$  values collected in PBDG are listed in Table SI-2. To compare the results in the three mesophases, the values of  $|\Delta\nu_Q|$  for **2** dissolved in PBG and the average of  $|\Delta\nu_Q|$ 's in the PBLG and PBDG versus  $^{2}\text{H}$  sites has been plotted (see Figure SI-5). The sets of  $^{2}\text{H}$  spectral data have been normalized to avoid experimental errors in sample preparation.<sup>16</sup> As seen, the three sets of quadrupolar data agree perfectly.

Conclusively, from the isotopic fractionation point of view, the results collected in PBLG, PBG, and PBDG samples demonstrate that (i) a true depletion effect (more or less marked) at one of the enantiotopic directions for both odd and even methylene groups exists all along the chain of this fatty acid, thus confirming the first results obtained from the BPTH analysis in CLC; (ii) the spectral discriminations of almost all enantioisotopomers are large enough for quantifying the ( $^{2}\text{H}/^{1}\text{H}$ )<sub>i</sub> ratios, thus to determine the full  $^{2}\text{H}$  isotopic profile of **2**.

**Determination of ( $^{2}\text{H}/^{1}\text{H}$ )<sub>i</sub> Ratios of Methyl Linoleate by Anisotropic NMR.** As almost all  $^{2}\text{H}$  sites are separated in the spectra recorded in mesophases (Figure 2a and b), a quantitative analysis to determine ( $^{2}\text{H}/^{1}\text{H}$ )<sub>i</sub> ratios along methyl linoleate **2** can now be made directly without resorting to chemical modification. In quantitative acquisition conditions (i.e.,  $T_R = 5T_1$ ), the surface of doublets for a given  $^{2}\text{H}$  site is theoretically proportional to the number of chiral or achiral monodeuterated isotopomers present in the mixture. The various quadrupolar doublets detected on the 2D map showed a good S/N ratio (from 11 on site 9 to 165 on site 1), and the surface measurement was performed by deconvoluting the signals (a sum of slices) extracted from the tilted 2D Q-COSY Fz map and using a curve-fitting algorithm.

The site-specific ( $^{2}\text{H}/^{1}\text{H}$ )<sub>i</sub> ratios (in ppm) are calculated from isotropic NMR values as follows:<sup>5</sup>

$$\left(\frac{^{2}\text{H}}{^{1}\text{H}}\right)_i^{\text{iso}} = \frac{P_{\text{ref}} m_{\text{ref}} M_s S_i (^{2}\text{H})}{P_i m_s M_{\text{ref}} S_{\text{ref}} (^{1}\text{H})_{\text{ref}}} \quad (2)$$

where  $P_i$  and  $P_{\text{ref}}$  are the stoichiometric numbers of hydrogen at site  $i$  and in the reference,  $S_i$  and  $S_{\text{ref}}$  are the areas of the signals at site  $i$  and reference, and  $M_s$ ,  $m_s$  and  $M_{\text{ref}}$ ,  $m_{\text{ref}}$  are the molecular weight and mass of the sample and the reference, respectively.

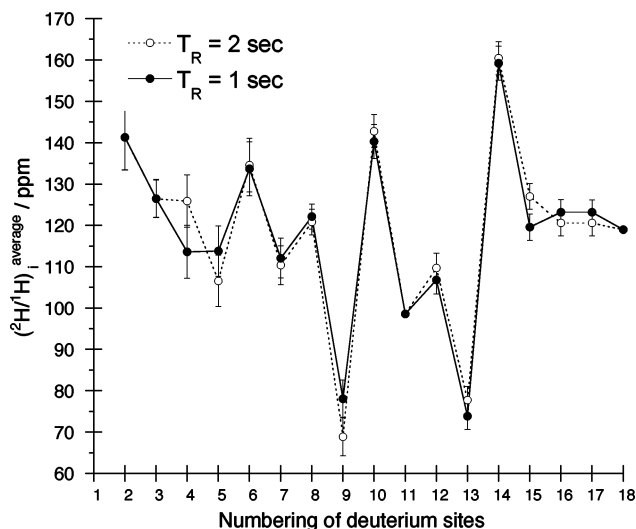


**Figure 3.** Comparison of averaged  $(^2\text{H}/^1\text{H})_i$  ratios measured for a recycling time of 1 and 2 s versus the  $^2\text{H}$  sites  $i$  (2–18) for FAME **2**. The error bars correspond to the SD error at each site. Methyl group 1 possesses extra botanical origin, and so it was not quantified. Note the odd/even effect along the chain.

As no calibrated internal reference (such as TMU) is added in the anisotropic sample, the  $(^2\text{H}/^1\text{H})_i$  ratios measured in PBLG, denoted  $(^2\text{H}/^1\text{H})_i^{\text{aniso}}$ , is derived from  $(^2\text{H}/^1\text{H})_i$  ratios determined by isotropic quantitative NAD NMR  $(^2\text{H}/^1\text{H})_i^{\text{iso}}$ , following eq 3:<sup>15</sup>

$$\left(\frac{^2\text{H}}{^1\text{H}}\right)_i^{\text{aniso}} = \left[\frac{(\% \text{ area})}{100} n \left(\frac{^2\text{H}}{^1\text{H}}\right)_i^{\text{iso}}\right] \quad (3)$$

where  $n$  is the number of equivalent deuterons contributing to the  $^2\text{H}$  isotropic signal. The values of  $(^2\text{H}/^1\text{H})_i^{\text{iso}}$  ratios used are reported in ref 10.

To verify the quantitative acquisition conditions (namely,  $T_R > 5T_1$ ) using a  $T_R$  of 1 s and optimizing the total acquisition time, the anisotropic NAD 2D spectrum of **2** has been recorded with a longer  $T_R$  (2 s).<sup>31</sup> This solution was preferred to that of classically measuring the  $T_1$  longitudinal relaxations by  $^2\text{H}$  inversion–recovery experiments in PBLG mesophases, which would require much more experimental time. The comparison of the averaged  $(^2\text{H}/^1\text{H})_i$  ratios for the sites 2–18 of **2**, is shown in Figure 3 and the numerical values are listed in Table SI-3. The data for  $T_R$  equal to 1 and 2 s clearly indicates that the  $(^2\text{H}/^1\text{H})_i$  ratios are identical within the standard deviation (SD). Consequently, a  $T_R$  of 1 s is sufficient to perform correct quantitative isotopic analyses in PBLG samples. This value of  $T_R$  has been kept for all NAD 2D experiments recorded in this work.

The accuracy of determining the  $(^2\text{H}/^1\text{H})_i^{\text{aniso}}$  values was evaluated by calculating the SDs from three identical NAD experiments. The SD values were found to vary between 2 and 8 ppm, values very similar to those typically determined in isotropic NAD NMR.

From the analysis of NAD 1D subspectra of **2** in PBLG, it is possible to measure the  $(^2\text{H}/^1\text{H})_i$  ratios for ethylenic sites 9, 10, 12, and 13, and for the pro-*S* and pro-*R* sites of prochiral groups 2, 3, 8, 14, and 15. Although the methylene sites 4, 16, and 17 are

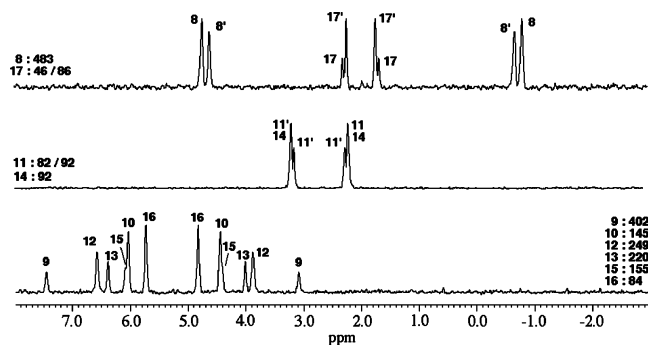


**Figure 4.** Three  $^2\text{H}\{-^1\text{H}\}$  1D subspectra extracted from the NAD 2D map of methyl linolenate **3** in PBLG/ $\text{CHCl}_3$ . The full series of 1D subspectra and zooms of 2D map are reported in the SI.

also enantioresolved, the overlap of quadrupolar doublets precludes a precise determination of  $(^2\text{H}/^1\text{H})_i$  ratios for these sites and the corresponding ratios were not determined. To overcome this problem, an optimization of the chiral mesophase is required by changing either the polypeptide, or the cosolvent, or both.

**Study of Methyl Oleate (1) and Methyl Linolenate (3).** The promising results obtained with **2** led us to extend the study to **1** and **3**, which possess one and three double bonds, respectively (Figure 1). The full series of NAD 1D subspectra extracted from the tilted *Q*-COSY Fz maps of **1** and **3** dissolved in PBLG/ $\text{CHCl}_3$  are given in Figure SI-6a and b. The assignment of doublets of **1** and **3** from the analysis of NAD 1D subspectra of **2** in PBLG was achieved on the basis of  $^2\text{H}$  chemical shifts, the  $(^2\text{H}/^1\text{H})_i$  ratios measured by  $^2\text{H}$  NMR in the liquid state and the assignments already made for methyl oleate **2**. Indeed, as we will highlight below, the orientational behavior of methylene groups 2–8 is similar for all FAMES. In other words, the magnitudes of  $\Delta\nu_Q$ 's are comparable for these sites, thus facilitating the assignment of the doublets for methylenes 4–8.<sup>33</sup> Moreover, the comparison of doublet intensities of methylene groups 15 and 17 between **1** and **2** provided crucial information for their assignment in **1** (see Figures 2 and SI-6a).

In the case of methyl linolenate **3**, the presence of a third double bond eliminates the  $^2\text{H}$  signals of methylenes 15 and 16 and deshields those of methylene group 17. Consequently, the assignment of methylenes presented in the second subspectrum (from top) in Figure 4 was easier than previously. In contrast, the assignment of six doublets corresponding to the ethylenic deuterons was not trivial and was achieved as follows. In a first step, we compared the quadrupolar splittings measured at ethylenic sites of **3** with those observed for **2** and **4** and assigned the doublets having the most similar splittings to sites 9 and 10. However, due to the geometry change of **3** compared to **2** and **4** in the C11–C18 portion (see below), the similarity in the magnitude of  $\Delta\nu_Q$ 's could not be applied unambiguously for doublets associated with ethylenic sites 12/13 and 15/16. To overcome this problem, we have associated, in a second step, the smaller signals with odd sites 13 and 15 since the  $(^2\text{H}/^1\text{H})_{\text{odd}}$  ratios are systematically depleted compared to the  $(^2\text{H}/^1\text{H})_{\text{even}}$  ratios in FAMES.<sup>10–14</sup> Then, as a KIE has been observed at site 15 but not at site 16 during the desaturation step performed by  $\Delta^{15}$  desatu-

(33) Canlet, C.; Merlet, D.; Lesot, P.; Meddour, A.; Loewenstein, A.; Courtieu, J. *Tetrahedron: Asymmetry* **2000**, *11*, 1911–1918.

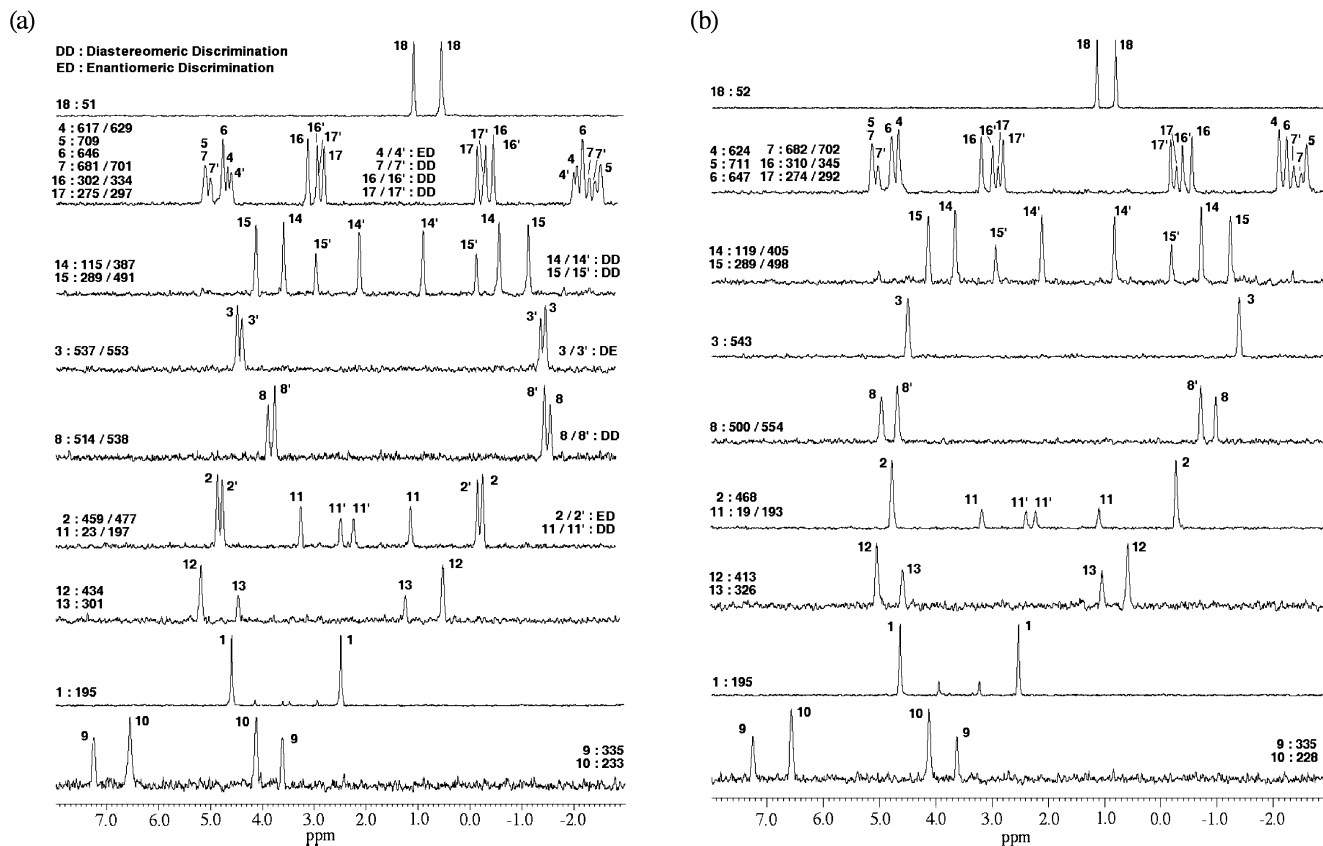


**Figure 5.** Series of  $^2\text{H}\{-^1\text{H}\}$  1D subspectra extracted from the tilted  $Q$ -COSY Fz map of methyl vernoleate **4** dissolved in (a) PBLG/ $\text{CHCl}_3$  and (b) PBG/ $\text{CHCl}_3$ . Zooms of 2D maps are reported in SI.

rise,<sup>34,35</sup> the  $(^2\text{H}/^1\text{H})_{16}$  should be higher than  $(^2\text{H}/^1\text{H})_{12}$ , another even ethylenic site, which is also subject to such a KIE. To confirm this, the ethylenic region of **3** has been compared with that of **2** (see Figure SI-11). Both the  $^2\text{H}$  chemical shifts and the trend in  $\Delta\nu_Q$ 's show some clear similarities between both external double bonds of **3** (sites 9/10 and 15/16) and the two double bonds of **2**.

In contrast with other FAMES, the  $^2\text{H}$  signals of methylene 11 of **3** are partly overlapped with those of 14 (Figure 4, third subspectrum from bottom) and it is difficult to assess directly whether or not spectral discrimination of the C–D enantiotopic directions occurs in these groups. At present, the difference between the  $\Delta\nu_Q$ 's measured on NAD 2D spectra of **3** recorded in the PBG and PBLG mesophases suggests that fortuitous doublet overlap occurs, hiding the enantiodiscrimination. Finally, as for compound **1**, the spectral enantiodiscrimination is observed on methylenes 2–4, but not on methylene groups 5–7 (see the discussion about the orientational behavior of FAMES **1**–**4**).

**Analysis of Methyl Vernoleate (4).** Vernoleic acid is found in the seed oils of several wild plants such as *Vernonia* sp. or *Euphorbia* sp and is very useful in the paint industry.<sup>36,37</sup> It is

biosynthesized from a linoleyl ester by a stereospecific oxidation of positions 12 and 13.<sup>38,39</sup> Compared with other FAMES, **4** is stereochemically interesting because it possesses two asymmetric carbon atoms (12*R* and 13*S*).<sup>38,39</sup> Hence, all pairs of C–D bonds in methylenes are diastereotopic, and thereby should be discriminated both in chiral and achiral mesophases.

Panels a and b in Figure 5 show the series of NAD 1D subspectra extracted from the tilted  $Q$ -COSY Fz map of **4** recorded in PBLG/ $\text{CHCl}_3$  and PBG/ $\text{CHCl}_3$ , respectively. As seen on NAD spectra, the largest spectral differentiations of diastereomeric directions occur for the C–D directions in methylene groups 11, 14, and 15, which are close to the asymmetric carbon atoms 12 and 13. For these sites, the separations of  $^2\text{H}$  doublets originate from both a difference of quadrupolar splittings and chemical shifts (doublets not centered). Logically, the diastereotopic directions in methylene groups 7, 8, 16, and 17, which are relatively remote from the stereogenic carbons (up to five bonds), show smaller spectral discriminations. No difference of chemical shift is measured for these, while the diastereotopic discrimination on the basis of a  $\Delta\nu_Q$  difference ( $\Delta\Delta\nu_Q$ ) is weaker than for previous sites.

Very striking is the differentiation of C–D directions for methylenes 2, 3, and 4 observed in PBLG but not in the PBG mesophase. This behavior is very intriguing and has never

(34) Ziani, L.; Lesot, P.; Meddour, A.; Courtieu, J. *Chem. Commun.* **2007**, 4737–4739.

(35) Savile, C. K.; Reed, D. W.; Meesapyodsuk, D.; Covello, P. S.; Buist, P. H. *J. Chem. Soc., Perkin Trans. 1* **2001**, 1116–1121.

(36) Daligault, F.; Reed, D. W.; Savile, C. K.; Nugier-Chauvin, C.; Patin, H.; Covello, P. S.; Buist, P. H. *Phytochemistry* **2003**, *63*, 739–744.

(37) Cuperus, F. P.; Derksen, J. T. P. In *Progress in New Crops*; Janick, J., Ed.; ASHS Press: Alexandria VA, 1996; pp 354–356.

(38) Heiko, T. B.; Becker, C.; Witzke-Ehbrecht, S. V. *Ind. Crops Products* **2005**, *21*, 257–261.

(39) Bafor, M.; Smith, M. A.; Jonsson, L.; Stobart, K.; Stymme, S. *Arch. Biochem. Biophys.* **1993**, *303*, 145–151.



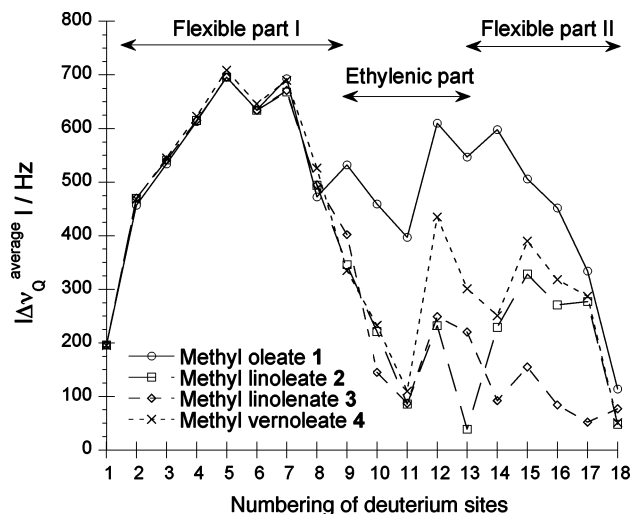


**Figure 6.** Comparison of the average of  $|\Delta\nu_Q$ 's values of analytes 1–4 dissolved in PBLG/ $\text{CHCl}_3$  versus the  $^2\text{H}$  sites.

previously been observed. It suggests that two kinds of enantio-discriminatory mechanisms may be acting simultaneously on a given solute, in particular if this possesses both stereogenic carbon(s) and long flexible chain(s). The first would be at the origin of the discrimination of deuterons close to asymmetric centers C12 and C13 (i.e., diastereotopic recognition mechanisms). The second would be associated with the discrimination of remote deuterons relative to the stereogenic carbons (i.e., enantiotopic recognition mechanisms). In fact, for this second case, the C–D directions are no longer “recognized” as diastereotopic due to their large distance relative to the asymmetric centers. In other words, from the point of view of these remote sites, the molecule behaves as a prochiral object interacting with the polypeptidic  $\alpha$ -helices. Consequently, only enantiotopic recognition mechanisms act and this leads to the spectral discrimination of C–D directions for these remote sites 2–4. Surprisingly, these two mechanisms might have opposite actions. Indeed in the case of site 8, the spectral discrimination is larger in PBG compared to PBLG mesophase (52 Hz instead of 23 Hz) where the two recognition mechanisms would a priori be active. This result raises some interesting questions (beyond the scope of this paper) on the role of the overall and local shape recognition phenomena of a long-chain chiral molecule dissolved in PBLG mesophases. It points out clearly that these physical phenomena are complex and that the recognition mechanisms could be tightly dependent on the stereospecificity of the various parts of a molecule.

**Qualitative Analysis of the Orientational Order of the Unsaturated Fatty Acids Studied.** In this last section, a qualitative analysis of the orientational behavior of FAMES 1–4 is presented. Using NAD 2D NMR, it has been recently demonstrated that isostructural rigid enantiomers dissolved in a given polypeptide CLC exhibit similar molecular orientational behaviors.<sup>33</sup> The present study of C-18 unsaturated fatty acids affords a good model to explore the orientational behavior of relatively similar flexible molecules.

Figure 6 shows the average of  $\Delta\nu_Q$ 's of compounds 1–4 in PBLG/ $\text{CHCl}_3$  versus the  $^2\text{H}$  site. The experimental values for sites 1–11 are very similar in FAMES 2–4. For analyte 1, a divergence

in  $\Delta\nu_Q$ 's is observed for sites 9–11, possibly due to the presence of a single double bond in the structure. In contrast, the values of averaged  $\Delta\nu_Q$ 's of sites 12–17 display weaker correlation between the four solutes. In other words, from an orientational ordering point of view, the four fatty acids studied behave as two independent flexible molecular fragments (sites 1–8 and sites 14–18) separated by a “rigid” linker (sites 9–13) created by the double bond(s) in 2 and 3 and the epoxide ring in 4. In fact, the presence of several linkers would de-correlate the orientational behavior of the two parts (C1–C11 and C14–C18) of these molecules. This argument could also explain why the discrimination mechanisms involved in methyl vernoleate 4 are different for sites close to the ester group compared with the others, as discussed above. In compounds 1–4, the first molecular fragment (sites 1–11) is identical and is characterized by seven  $-\text{CH}_2-$  rotors. This part of the molecule is probably oriented identically inside the mesophase, as if the molecule was “rigid”. Molecular modeling calculations (see Figure SI-12) using a semiempirical method (AM1)<sup>40,41</sup> have shown that the structure of the C1–C11 fragment for the lowest energy conformer was superimposable for molecules 1–4. Hence, we can reasonably assume that the conformational dynamics of this first fragment is very similar, both in the gas phase and in oriented solvent. Indeed, it has been shown that PBLG mesophases do not modify significantly the conformational distribution function of flexible solutes.<sup>42</sup> Assuming that the conformational distribution of the C1–C11 part for 1–4 is identical, the molecular long axis of these solutes should be oriented more or less parallel along the PBLG fibers, and the orientational behaviors of the flexible part (C1–C11) should be very similar. If we now superimpose the (C1–C11) parts of the molecules, we observe that the long axis for the second flexible fragment, C14–C18, is more or less bent relative to the long axis associated with the C1–C11 fragment. This molecular bending depends on the number of rigid linkers, namely, the double bonds (one, two, or three) or epoxide ring. The most bent molecule is methyl linolenate 3. This situation would lead to changes in the orientational behavior for  $^2\text{H}$  sites in the C14–C18 fragment in FAMES 1–4. Experimentally, the magnitudes of  $\Delta\nu_Q$ 's are different between FAMES 1–4. However, at least for solutes 2–4, the profile (general trend) of  $\Delta\nu_Q$ 's along the chain appears very similar (Figure 6). The very close values of quadrupolar splittings for the methyl group (C18) in 1–4 are not very informative due to the averaging effect associated with the free rotation of the methyl group.

**Assignment of Stereochemical Stereodescriptors in Anisotropic NAD Spectra of FAMES.** The assignment of pro-*R*/pro-*S* stereodescriptors of quadrupolar doublets at each discriminated methylene site in FAMES 1–4 is an essential step in obtaining information about the reaction mechanisms of the enzymes of the FAD superfamily involved in the modification of stearoyl (C-18, saturated) to produce, via linoleoyl, either C-18 polyunsaturated

(40) Lee, M.; Lenman, M.; Banas, A.; Bafor, M.; Singh, S.; Schweizer, M.; Nilsson, R.; Liljenberg, C.; Dahlqvist, A.; Gummesson, P. O.; Sjö Dahl, S.; Green, A.; Szymme, S. *Science* **1998**, *280*, 915–918.

(41) Hyperchem<sup>TM</sup>, Professional 6.1, Hypercube, Inc, 1115 NN 4th St., Gainesville, FL, 32601.

(42) Dewar, M. J. S.; Dieter, K. M. *J. Am. Chem. Soc.* **1986**, *108*, 8075–8086.

fatty acid, such as linolenoyl and conjugated linolenoyl, or C-18 oxidized fatty acids, such as vernoleoyl. However, no simple relationship exists between the magnitude of  $\Delta\nu_Q$ 's measured on NAD spectra and the assignment of pro-*R*/pro-*S* stereodescriptors for a given prochiral molecule, making it impossible to establish a direct correlation.<sup>16,43</sup> Moreover, this assignment at a given methylene site is a priori not valid for another site

Nevertheless, it is possible to assign the doublets to enantiomeric monodeuterated isotopomers at methylene groups in **2** on the basis of the stereochemical assignments made on the methylene sites, 4 and 5, of BPTH, and the mechanism of stearoyl biosynthesis. Since the elongation of the fatty acid chain always follows the same process (addition of two carbons from acetate in each cycle of the FAS activity), the origin and prochirality of hydrogen at each type of methylene site (odd or even) is the same.<sup>44</sup> Thus, each hydrogen is introduced with a defined pro-*R*/pro-*S* stereochemistry at the odd and even methylenes. Hence, the correct assignment of the stereodescriptors, pro-*R*/pro-*S*, to the lowest or highest intensity doublet of a single methylene site (even or odd), will be extendable to other methylene groups along the fatty acid chain.

Previously, the study on BPTH obtained by chemical modification of **2** showed clearly that  $(^2\text{H}/^1\text{H})_{\text{pro-S}}$  ratios were lower than the  $(^2\text{H}/^1\text{H})_{\text{pro-R}}$  ratios at even and odd methylenes (sites 4 and 5).<sup>15</sup> As the BPTH has the same botanical origin (safflower) as methyl linoleate **2**, the isotopic fractionation relative to sites 4 and 5 in BPTH is therefore the same as for sites 16 and 17 in methyl stearate, hence in methyl linoleate (see Figure 7a–c). Therefore, we can confidently predict that the  $(^2\text{H}/^1\text{H})_{\text{pro-S}}$  ratio is always smaller than the  $(^2\text{H}/^1\text{H})_{\text{pro-R}}$  ratio at each odd and even methylene (15 to 2). Formally, this argument is only valid in the case of methyl stearate, because, as seen in Figure 7b, the stereochemistry of deuterium sites located in front of the molecular symmetry plane is always the same along the chain, according to the CIP rules (as in BPTH). In contrast, this stereochemical characteristic is not true in the case of methyl linoleate because for methylene groups 6–8 the stereochemistry of deuterium sites located in front of the plane of symmetry are inverted compared with in methyl stearate (according to the CIP rules) due to the presence of the double bond in position 9–10. The pro-*R*/pro-*S* assignments of quadrupolar doublets associated with enantiotopic directions at each enantio-discriminated methylene group of **2** are reported in Figure 7d. Except for the methylene site 8 in **2**, we have assigned the stereodescriptors, pro-*R*/pro-*S*, to the lowest or highest intensity doublets displayed on NAD 1D subspectra. For methylene 8, the situation is inverted compared with other methylenic sites as the CIP rules are applied here.

Interestingly it can be noted that for the C2–C7 fragment, the inner doublet at odd and even methylene sites corresponds to the pro-*S* direction while the opposite situation exists for the C14–C17 fragment. This finding suggests that the two flexible parts of the molecule at each side of the linker (two double bonds) enantioselectively interact very differently with the PBLG fibers,

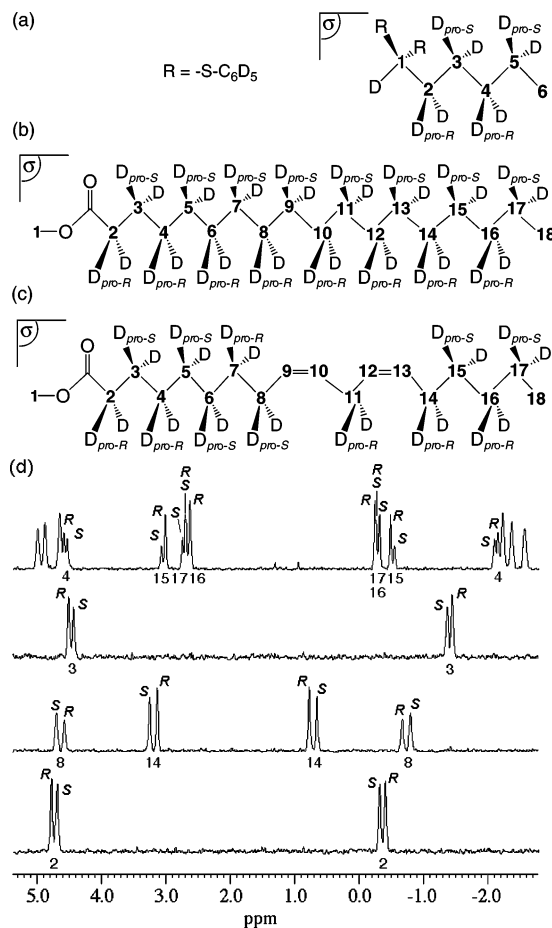


**Figure 7.** (a–c) Assignments of pro-*R* and pro-*S* stereodescriptors along the chain of (a) BPTH, (b) of methyl stearate, and (c) methyl linoleate **2**. All molecules are assumed to be perdeuterated. (d) *R/S* assignment of quadrupolar doublets of methylene groups of **2** showing spectral enantiodiscriminations (according to the CIP rules).

thus inducing the inversion of the inner and outer doublets relative to their stereochemistry. In this framework, the result obtained for C8 is not in contradiction with the behavior of other methylenes in the C2–C7 fragment since the stereochemical inversion for the lowest and highest intensity doublets is only an artifact due to the CIP rules. From the molecular geometry point of view, the deuterium sites defined as pro-*R* in methylene groups 6 and 8 in **2** correspond to the deuterium sites defined as pro-*S* in stearate (see Figure 7b and c), both on average being located in front of the molecular symmetry plane. A reversal of this situation exists for the methylene group 7.

The variation of the  $(^2\text{H}/^1\text{H})_S$  and  $(^2\text{H}/^1\text{H})_R$  ratios versus each methylene site of **2** is shown in Figure 8. As can be seen, the difference between the enantiotopic sites varies between 4 (site 2) and 91 ppm (site 15).

For FAMES **1**, **3**, and **4**, the same strategy should be applicable for assigning the stereodescriptors associated with doublets for each methylene group showing spectral enantiodiscrimination. Using the same botanical origin, this assignment would now be possible and achievable by comparing each FAME with the corresponding methyl linoleate isolated from the same plant. The isolation of FAMES from the same botanical origin is currently being carried out in order to perform this comparison.

(43) Emsley, J. W.; Lesot, P.; Merlet, D. *Phys. Chem. Chem. Phys.* **2004**, *6*, 522–530.

(44) Aroulanda, C.; Lesot, P.; Merlet, D.; Courtieu, J. *J. Phys. Chem. A* **2003**, *107*, 10911.



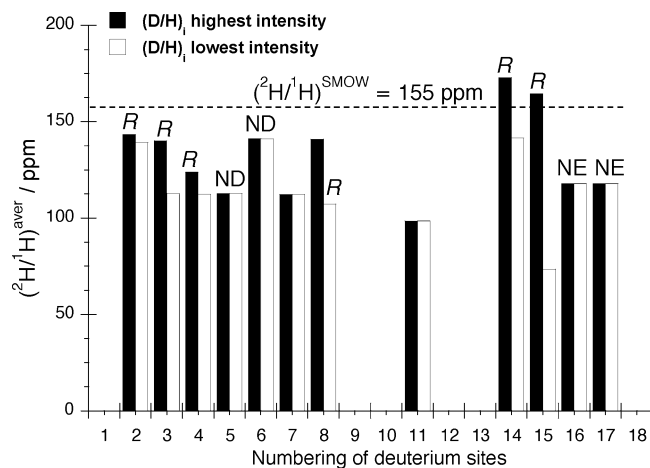


**Figure 8.** Comparison of ( $^2\text{H}/^1\text{H}$ )<sub>S</sub> and ( $^2\text{H}/^1\text{H}$ )<sub>R</sub> ratios versus the methylene sites. ND and NE stand for “no discrimination” and “no evaluation” of sites due to very important overlap of peaks. SMOW is the standard mean ocean water value.

## EXPERIMENTAL SECTION

**Materials.** Methyl oleate (**1**) (from *Helianthus annuus*, sunflower), methyl linoleate (**2**) (from *Carthamus tinctorius*, safflower), and methyl linolenate (**3**) (from *Linum usitatissimum*, flax) were purchased from Sigma-Aldrich. Methyl vernoleate (**4**) (from *Vernonia galamensis*, sunflower family) was extracted following the procedure previously developed.<sup>15</sup> PBLG has a degree of polymerization of 782 ( $M_w \approx 171\,300$ ) (Sigma-Aldrich). Chloroform (stabilized with ethanol) was dried using molecular sieves prior to be used.

**Sample Preparation.** The standard procedure to prepare samples using 5-mm NMR tubes was described previously.<sup>15,19</sup> In this study, the PBLG/ $\text{CHCl}_3$  samples were prepared by dissolving 100 mg of solute in  $\sim 100$  mg of PBLG and 650 mg of dry chloroform. This gives a concentration (% w/w) of polymer of 11.8, and the concentration in monodeuterated isotopomers for solutes **1** to **4** is  $\sim 60$   $\mu\text{M}$ .

The exact compositions are listed in Table SI-4. To reach the best possible spectral resolution, several cycles of centrifugation and rehomogenization of the sample were carried out to remove concentration gradients. This operation is crucial because a lack of macroscopic homogeneity strongly affects the line widths of NAD spectra, hence the S/N ratio for the solute signals. NMR tubes were fire-sealed to avoid solvent evaporation.

**NMR Measurements.** NAD 2D NMR spectra were recorded on a Bruker Avance II 600 MHz NMR spectrometer (14.1 T) equipped with a 5-mm selective  $^2\text{H}$  cryogenic probe (92.1 MHz). All NAD 2D NMR experiments were recorded applying the WALTZ-16 sequence to decouple protons and without  $^{19}\text{F}$  lock. The temperature of all NMR tubes was regulated carefully at 300 K.

Unless otherwise specified, the NAD 2D experiments were recorded using 96 FIDs for each  $t_1$  increment and a 2D matrix of  $1530$  ( $t_2$ )  $\times$   $512$  ( $t_1$ ) data points. The same spectral width (1700 Hz) was used in both dimensions. The recycling time for each scan was of 1 s, leading to a total acquisition time of  $\sim 15$  h. Exponential filtering ( $\text{LB} = 1\text{--}1.5$  Hz) was applied in both

dimensions. The 2D maps were zero-filled to  $2048$  ( $t_1$ )  $\times$   $2048$  ( $t_2$ ) data points prior to 2D FT and then symmetrized and tilted. Other details are given in the figure legends. The area measurement was performed using a curve-fitting algorithm of a complex least-squares treatment of the  $^2\text{H}$  NMR signal (Perch NMR software).<sup>45</sup>

## CONCLUSION

The potential of NAD 2D NMR spectroscopy in polypeptide chiral liquid crystals for studying the isotopic fractionation of whole C-18 unsaturated fatty acids (**1–4**) has been explored. The significant increase of the sensitivity resulting from the use of a 14.1-T spectrometer equipped with  $^2\text{H}$  cryoprobe has considerably improved the analytical potential of this approach, giving access to detailed information on ( $^2\text{H}/^1\text{H}$ )<sub>i</sub> ratios that was inaccessible by classical methodology.

The S/N ratios reached in this investigation show clearly that the accuracy of ( $^2\text{H}/^1\text{H}$ )<sub>i</sub> ratio measurement has been considerably improved compared with our early study in BPTH<sup>15</sup> and that a precision close to that of classical isotropic techniques can be obtained.

The results presented here show a significant progress in measuring the  $^2\text{H}$  fractionation in C-18 unsaturated fatty acids in CLCs and how unique information inaccessible by isotropic classical means can be efficiently revealed.

Attention has been mainly focused on linoleic acid, a key fatty acid from which numerous other fatty acids are biosynthesized including linolenic acid, vernoleic acid, and conjugated linolenic acids. The study shows that the ( $^2\text{H}/^1\text{H}$ )<sub>i</sub> ratios at nearly all sites of such C-18 fatty acids can be determined without need to resort to chemical modification. Others FAMES such as **1**, **3**, and **4** have been also successfully tested, thus showing that the method can be effectively applied to numerous fatty acids.

NAD 2D NMR in CLCs provides an important advance, as it removes the risk to introducing non-natural  $^2\text{H}$  fractionation during the chemical modification and greatly reduces the time spent in sample preparation. Moreover, the discrimination of the enantiotopic directions of almost all methylene and ethylenic sites is determined. Thus, it is possible to study the nonstatistical distribution of deuterium in terms of the origins of hydrogen and the KIEs, which occurs during the elongation steps of the fatty acid chain. In turn, this makes it feasible to probe the differences in KIEs associated with desaturases, conjugases, or epoxidases, all of which use linoleate esters as substrates and modify this C-18 chain.

However, as seen, in sites 5–7 and 11 in **2**, 5–7 in **3**, and 5 and 6 in **4**, the PBLG/ $\text{CHCl}_3$  mesophase does not discriminate the enantiotopic directions of all methylene sites. Furthermore, in some cases (for instance sites 16 and 17 in **2**; 10 and 15, 11 and 14 in **3**), the quadrupolar doublets strongly overlap, precluding an accurate determination of these ( $^2\text{H}/^1\text{H}$ )<sub>i</sub> ratios. To

(45) (a) Sedgwick, B.; Cornforth, J. W.; French, S. J.; Gray, R. T.; Kelstrup, E.; Willadsen, P. *Eur. J. Biochem.* **1977**, *75*, 481–495. (b) Okuda, S. *GC-MS News* **1985**, *13*, 94–100.

(46) Perch NMR Software, version 1/2000 (Evaluation version), University of Kuopio, Finland.

resolvethese remaining difficulties and to achieve discrimination of all enantiotopic directions, other polypeptide oriented systems are currently tested.

#### **ACKNOWLEDGMENT**

The authors thank Dr. Richard J. Robins for critically reviewing the manuscript. V.B. gratefully thanks the French MNESR for a Ph.D. grant.

#### **SUPPORTING INFORMATION AVAILABLE**

Additional information as noted in text. This material is available free of charge via the Internet at <http://pubs.acs.org>.

Received for review November 29, 2007. Accepted January 30, 2008.

AC702443B